Electronic Supplementary Information

Redox insights and OER activity in 3D-MOFs: The role of alkali metal ions

Susanta Dinda,[a] Arun Karmakar,[b] Debajyoti Ghoshal,[a]* and Subrata Kundu[b]*

[a]Department of chemistry, Jadavpur University, Jadavpur, Kolkata-700032

[b]Materials Chemistry Laboratory for Energy, Environment and Catalysis, Electrochemical

Process Engineering (EPE) Division, CSIR-Central Electrochemical Research Institute

(CECRI), Karaikudi-630003, Tamil Nadu, India.

E-mail: debajyoti.ghoshal@jadavpuruniversity.in; skundu@cecri.res.in

This file contains 16 pages in which the details of chemicals, synthesis, physical characterization, electrodes fabrications, material preparation for different characterizations, data for OER, comparative electrocatalysis data are given in detail.

Number of figures: 11

Number of table: 4

Contents

Experimental section

Chemicals

Immensely fresh $Co(NO_3)_2 \cdot 6H_2O$, imidazole, dichloromethane, tetrabutylammonium chloride and 2,6-pyridine carboxylic acid have been acquired from the Sigma-Aldrich Chemical Co. All other reagents and solvents have been bought from commercial sources and used except further clarification. di(1H-imidazol-1-yl)methane[1] have been synthesized by a reaction between dichloromethane and imidazole in presence potassium hydroxide and tetrabutyl alumium bromide(TBAB) at 40^0C in inert atmosphere condition. Na_2-2,6-pyridine dicarboxylate (2,6-pc) had been synthesized by the sluggish collation of solid NaOH to the analogous acids (H_2-2,6-pc) in water in a 2:1 ratio and allowed to evaporate until dryness.

Synthesis of CP 1 (Set-1)

The slightly modified method has been used as reported[2] earlier, here aqueous solution of Na_2-2,6-pyridine dicarboxylate (2,6-pc) (1 mmol, 213 mg) was slowly mixed with a methanolic solution (20 mL) of di(1H-imidazol-1-yl)methane (1 mmol, 148 mg) and stirred for 20 min to mix well. Slowly and carefully, 3ml aqueous solution of Co(II) from 20 mL aqueous solution of $Co(NO_3)_2 \cdot 6H_2O$ (1 mmol, 0.291 g) was layered with 6 mL of the aforesaid mixed-ligand solution by using 5 mL of buffer (1:1 water/ MeOH mixture) allowed to reacts through slow diffusion method. At the juncture of the solution pink block-shaped single crystals has been appeared in the layer tube after 15 days. Yield: 90%. Elemental analysis, calculated for $C_{14}H_{13}CoN_5O_5$ (390.21): C 43.49; H 2.84; N 18.12; O 20.70; Co 15.25. Found: C 43.41; H 2.80; N 18.10; O 20.65; Co 15.20.

Synthesis of K@Co-carbonate MOF (Set-2)

The layer tube of compound **1** has been over saturated by solid potassium carbonate (K_2CO_3) then 3 ml methanolic solution of trans-1,2-bis(4-pyridyl)ethylene ligand (bpe) (out of 20 ml solution of 1 mmol, 0.182 g) has been added, shacked for 5 minutes. The resulting solution stay for 7 days,

magenta color crystals have been appeared throughout the tube, collected and performed X-ray diffraction analysis, found identical with the previously reported compound[3]. Yield: 95%. Elemental analysis, calculated for $K_2C_2H_4CoO_{10}$ (325.15): C 8.81; O 50.42; K 24.34; Co 18.57. Found: C 8.75; O 50.35; K 24.28; Co 18.50.

Synthesis of K@Co-2,6-pc MOF (Set-3)

The synthesis process is exactly same except instead of over saturation of reaction solution by K_2CO_3 of compound **1** unsaturation (below saturation) of reaction solution by K_2CO_3 has been used, black color crystals have been appeared at the bottom of the tube, collected and performed X-ray diffraction analysis, which is similar to the previously reported compound[4]. Yield: 93%. Elemental analysis, calculated for $K_2C_{14}H_{20}CoN_2O_{15}$ (593.34): C 29.69; H 1.05; N 4.95; O 44.47; K 13.82; Co 10.42. Found: C 29.60; H 1.04; N 4.90; O 44.40; K 13.75; Co 10.35.

Physical measurements.

Elemental analysis. Elemental analyses (C, H, N) have been performed using a Heraeus CHNS elemental analyzer. FT-IR spectra have been obtained on a Perkin Elmer spectrometer (Spectrum II) with the samples.

Thermogravimetric analysis. PerkinElmer STA8000 thermal analyzer has been used for thermogravimetric analysis (TGA) with a ramp rate of 5 °C/min from room temperature to 600 °C under nitrogen flow.

Fourier transform infrared spectroscopy. Infrared spectra were collected on a Perkin Elmer Spectrum Two Fourier transform infrared spectrometer fitted with an attenuated total reflectance accessory comprised of a single reflection diamond crystal. A wavenumber range spanning 4000–400 cm^{-1} was recorded.

Powder x-ray diffraction. Powder X-ray diffraction (PXRD) data were collected on a Bruker D8 Discover instrument with Cu-Kα radiation (λ = 1.5406 Å), operating at 40 kV and 40 mA.

TEM and XPS

The synthesized MOFs were examined using Talos F-200-S with HAADF elemental mapping and HR-TEM (TecnaiTM G2 TF20) operating at a 200 kV accelerating voltage. The investigation was conducted using Theta Probe AR-XPS (Thermo Fisher Scientific, UK) X-ray photoelectron spectroscopy.

Electrochemical characterization.

AURT-M204 connected with three cell configurations has been exploited for all electrochemical characterizations. The Hg/HgO reference electrode was purchased from the CH instrument. The Pt-coil was purchased from Metroohm and was used as the counter electrode. The entire potential data was collected by using Hg/HgO as the reference electrode, which was converted into a Reversal hydrogen electrode (E_{RHE}) scale by the Nernst equation

$$E_{RHE} = E_{ref} + 0.059 \times 14 + 0.098 \dots\dots\dots\dots\dots S1$$

Over potential (η) value of pristine CoFe- LDH and different loading of Ru@Cofe-LDH (1%, 3%, and 5%) at benchmarking current density of 10 mA/cm^2 is calculated by the following equation:

$$\eta = E_{RHE} - 1.23 \text{ V (for OER)} \dots\dots\dots\dots\dots S2$$

$$\eta = 0 - E_{RHE} \text{ (for HER)} \dots\dots\dots\dots\dots S3$$

Tafel slope was calculated from 100 % iR-drop free LSV polarization data followed by fitting η vs log (current density) using the Tafel equation

$$\eta = \beta \cdot \log(j/j_0) \dots\dots\dots\dots\dots S4$$

where β signify the Tafel slope value, j signifies the current density, and j_0 is the exchange current density.

To prepare various CP and Co_3O_4 modified electrode, ink is made by mixing 3mg of catalyst powder with 200μl isopropanol + 50μl Nafion + 750μl DI water. The ink is sonicated for 30 min until fully dispersed. The as-prepared ink (34.5 μL) is drop-casted over Carbon Cloth (CC) and is dried in an oven at 60 °C for overnight.

Determination of surface concentration, charge over the electrode surface and TOF values of all four catalyst from the redox features of CV:

Calculated area associated with the reduction of Co^{2+} to Co^{3+} of **Set-3** = 0.0000634 VA

Hence, the associated charge is = 0.0000634 VA / 0.005 Vs-1

$$= 0.01268 \text{ As}$$

$$\mathbf{= 0.01268 \text{ C}}$$

Now, the number of electron transferred is = 0.01268 C / 1.602 ×10^{-19}

$$\mathbf{= 7.91 \times 10^{16}}$$

Since, the oxidation of Co^{2+} to Co^{3+} is a single electron transfer reaction, the number of electrons calculated above is the same as the number of surface-active sites.

Hence, the number of Co participate in OER is = **7.91 × 10^{16}**

Determination of Turnover Frequency (TOF) from OER Current Density TOF in our study was calculated assuming that the surface-active Co atoms that had undergone the redox reaction just before onset of OER only participated in OER electrocatalysis. The corresponding expression is,

$$TOF = \frac{j \times N_A}{n \times F \times \tau} \ldots\ldots\ldots\ldots\ldots \text{(S5)}$$

Where, j = current density N_A= Avogadro number F = Faraday constant n = Number of electrons Γ = Surface concentration.

Hence, we have,

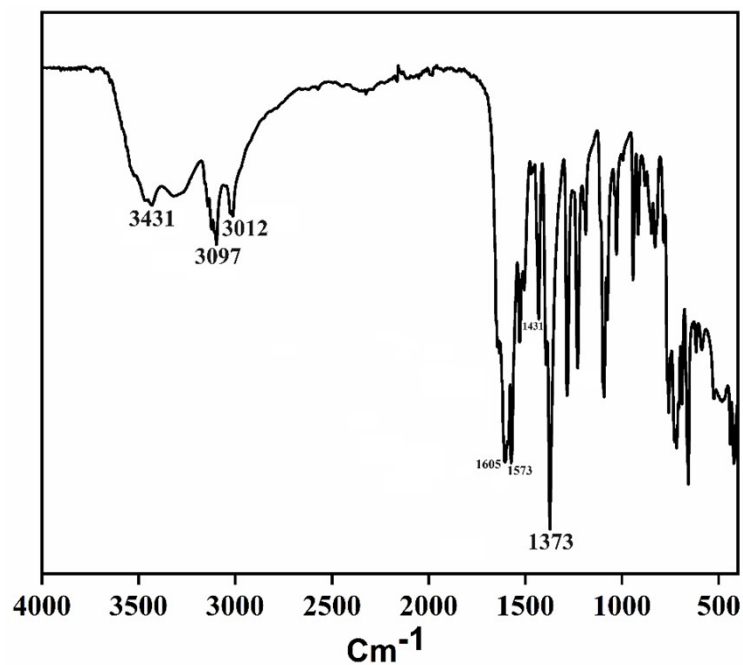$TOF_{1.6 \text{ V}}$ = [(0.0997) (6.023× 10^{23})] / [(96485) (4) (6.367 × 10^{15})]

= 1.96 sec⁻¹

Fig. S1. IR spectra of Set-**1.** IR spectra (KBr pellet, 4000−400 cm⁻¹): ν(O−H), 3431 (stretch); ν(C−H), 3097 (stretch); ν(C−H, alkane), 3012 (stretch) and 1431 (bending); ν(C−C) 1573 (stretch); ν(C−O, carboxylate), 1605 (stretch) and ν(C−N), 1373 (stretch).
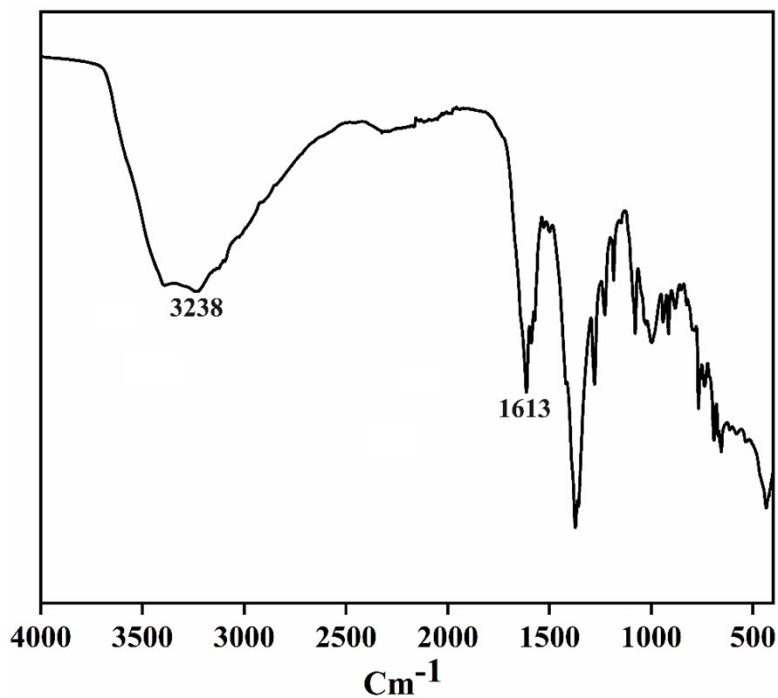

Fig. S2. IR spectra of Set-**2.** IR spectra (KBr pellet, 4000−400 cm⁻¹): ν(O−H), 3238 (stretch); ν(C−O, carbonate), 1613 (stretch).

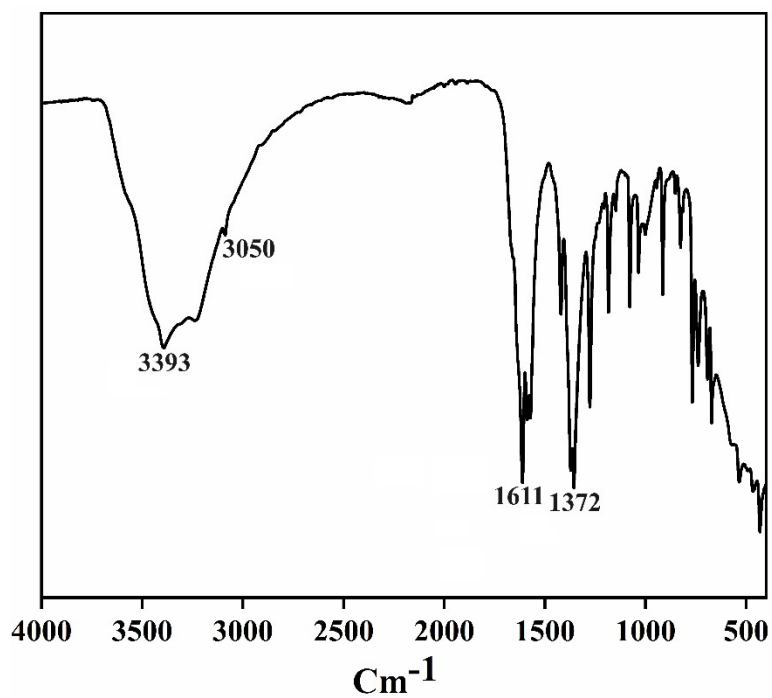**Fig. S3.** IR spectra of Set-**3.** IR spectra (KBr pellet, 4000−400 cm^{-1}): ν(O−H), 3393 (stretch) ν(C−H), 3050 (stretch) ν(C−O), 1611 (stretch) and ν(C−N), 1372 (stretch).
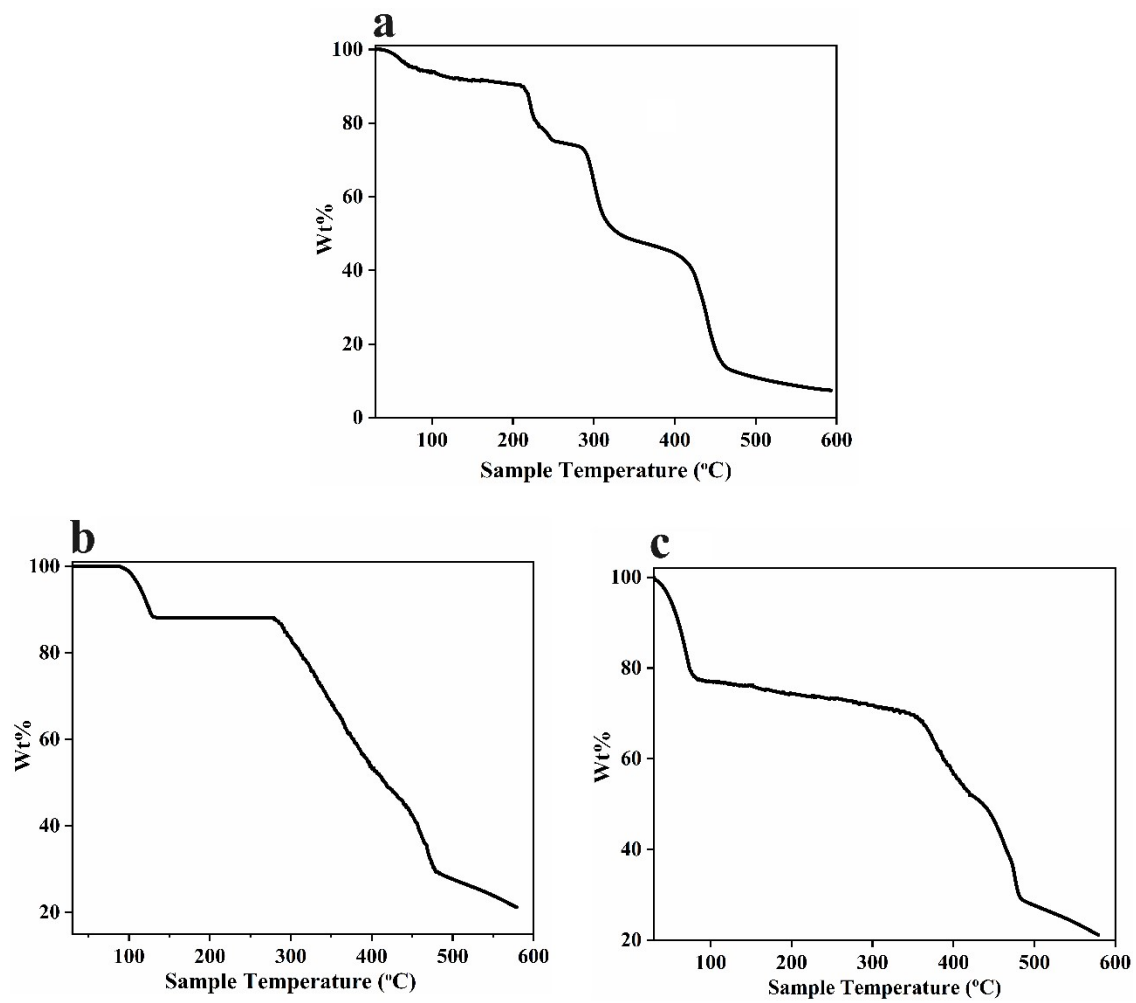
Fig. S4. Thermogravimetric analysis of Set 1 **(a)** Set 2 **(b)** Set 3 **(c).**

Table S1. Selected Bond Lengths (Å) of Set-**2** MOF.

Co1-O1	2.0693(18)	Co1-O1W	2.129(2)
Co1-O2W^a	2.1352(19)	Co1-O2W	2.1352(19)
Co1-O1^a	2.0693(18)	Co1-O1W^a	2.129(2)
K1-O2	2.704(2)	K1-O2W	2.804(2)
K1-O3	2.740(2)	K1-O1	2.810(2)
K1-O1W	3.019(2)		

a =1-x,2-y,1-z

Table S2. Selected Bond Lengths (Å) of Set-**3** MOF.

Co1-O1	2.161(3)	Co1-N1	2.035(4)
Co1-O1^b	2.161(3)	Co1-O4^b	2.160(3)
Co1-N1^b	2.035(4)	Co1-O4	2.160(3)
K1-O2W	2.646(8)	K1-O3	2.749(4)
K1-O3^a	2.749(4)	K1-O4W^b	2.811(4)
K1-O4W^c	2.811(4)	K1-O1W^h	2.970(4)
K1-O1W^j	2.970(4)	K2-O1W	2.813(4)
K2-O1W^b	2.813(4)	K2-O3^g	2.883(4)
K2-O3W^g	2.986(6)	K2-O3^k	2.883(4)
K2-O3W^k	2.986(6)		

a =1/2-x,1-y,z, b =x,3/2-y,1/2-z, c =1/2-x,-1/2+y,1/2-z, g =1/2+x,y,1-z, h =1-x,-1/2+y,1/2+z,

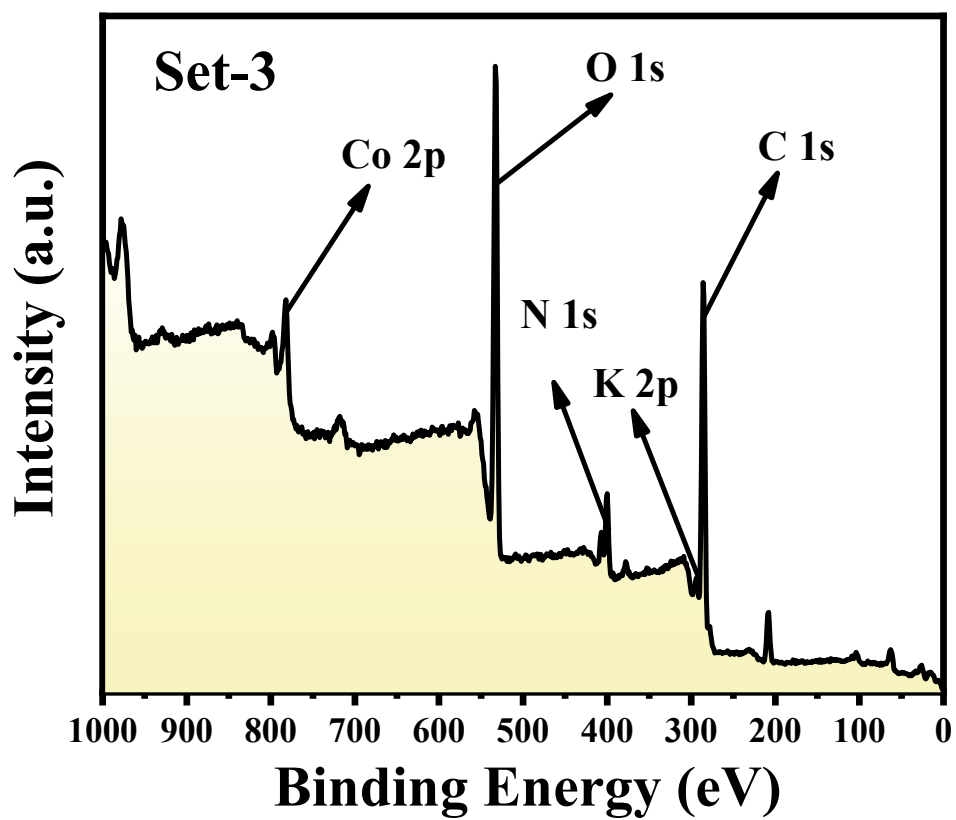k =1/2+x,3/2-y,-1/2+z.

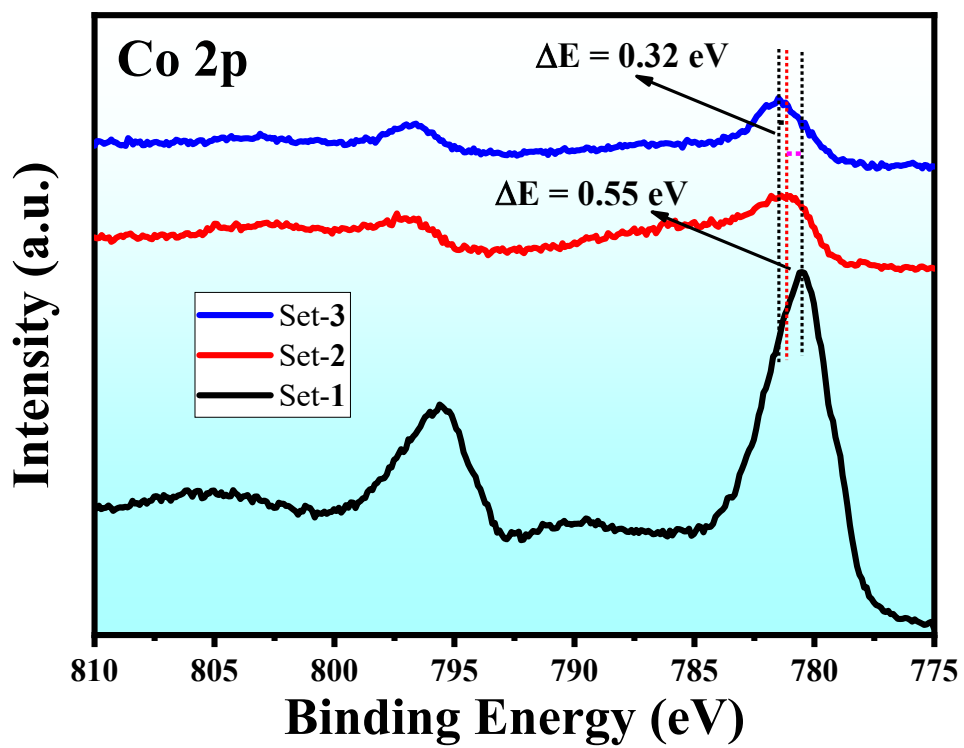**Fig. S5.** XPS survey spectrum of Set-**3** MOF.

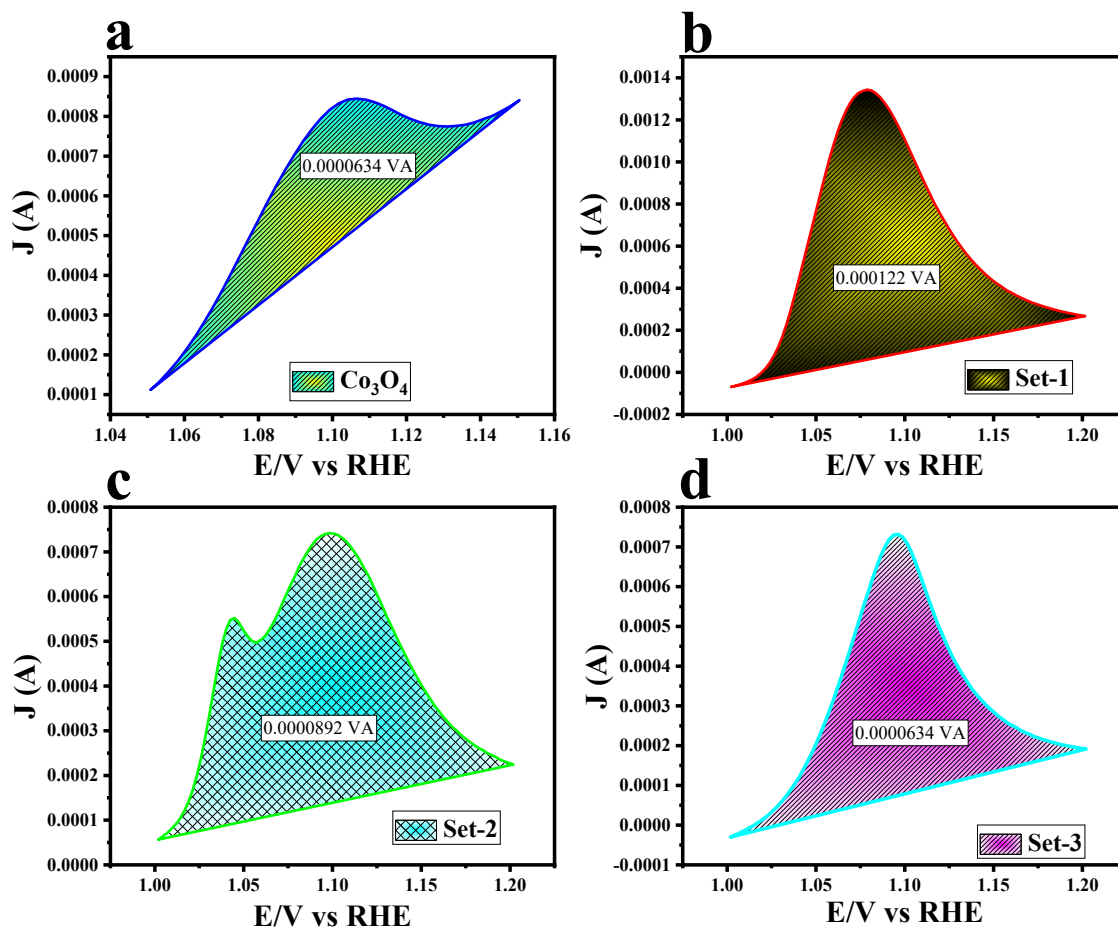**Fig. S6.** XPS spectrum of Co 2p orbital of Set-1, Set-2, and Set-3 catalyst.

Fig. S7. (a-d) Anodic redox response for Co_3O_4, Set-**1**, Set-**2** and Set-**3** compounds.

Table S3. Comparative electrochemical outcomes of pristine Co_3O_4 and various Set-**1**, Set-**2** and Set-**3** compounds.

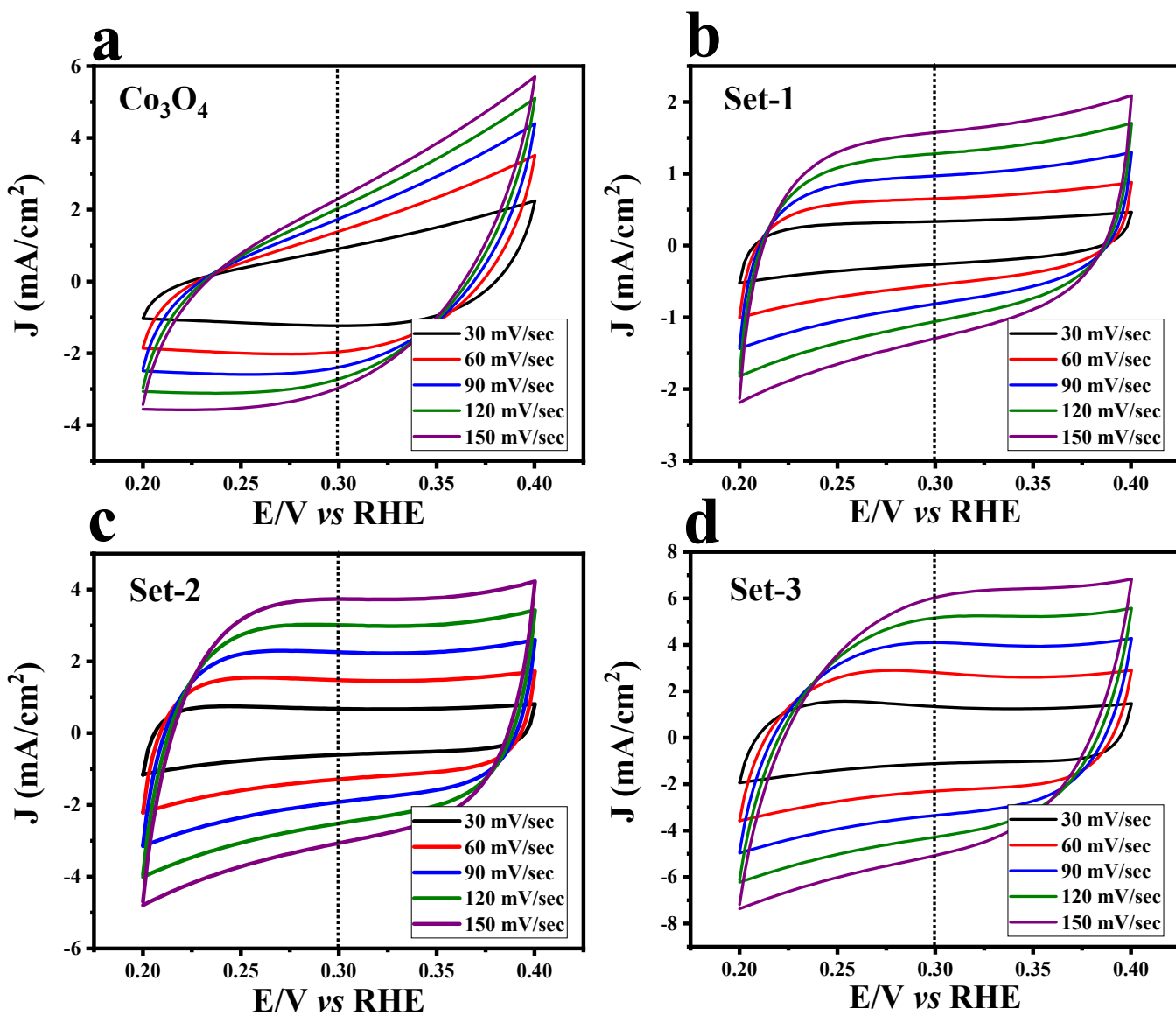| Sl. No.	Compound	Potential (V)	Reduction surface area (VA)	Charge over the electrode surface (C)	Number of active Co sites	TOF (sec^{-1})
1	Co_3O_4	1.53	0.0000634	0.01268	7.91×10^{16}	0.02031
		1.55				0.02879
		1.6				0.07315
2	Set-1	1.53	0.000122	0.0244	1.52×10^{17}	0.02203
		1.55				0.0418
		1.6				0.28024
3	Set-2	1.53	0.0000892	0.01784	1.11×10^{17}	0.1037
		1.55				0.19928
		1.6				0.777
4	Set-3	1.53	0.0000634	0.00791	7.91×10^{16}	0.23483
		1.55				0.49489
		1.6				1.96576

Fig. S8. (a-d) Cyclic voltametric response for Co_3O_4, Set-**1**, Set-**2** and Set-**3** compounds with respect of different scan rate value to have a knowledge about double layer capacitance (C_{dl}) information.

Table S4. A comparison of electrocatalytic OER performance of Set-**3** MOF to that of contemporary materials.

| Sl. No.	Material	Overpotential (mV)@10 mA/cm^2	Tafel Slope (mV/dec)	TOF value (S^{-1})	Reference
1.	CoCd-MOF	353@1mA/cm^2 (pH 13.0)	110	3.314×10^{-2}	5
2.	NG-CoSe2	366	40	0.03	6
3.	MOF-2	370@1mA/cm^2 (pH 13.0)	101.9	0.6	7
4.	Co-WOC-1	390@1 mA/cm^2 (pH 13.0)	128	0.05	8
5.	CSMCRI-10	396 (pH 14.0)	102	0.03	9
6.	HFC Co$_3$O$_4$	400 (pH 14.0)	70	1.67×10^{-2}	10
7.	Co-TpBpy	400@1 mA/cm^2 (pH 7.0, buffer)	59	0.23	11
8.	UTSA-16	408 (pH 14.0)	77	-	12
9.	Co$_2$-MOF@Nafion	460@2 mA/cm^2 and 537@5 mA/cm^2 (pH 7.0)	105±5	0.026	13
10.	Co-ZIF-9	510@1 mA/cm^2 (pH 13.4)	193	1.76×10^{-3}	14
11.	NU-1000 MOF Thin Film	566 (pH 11.0, buffer)	90	1.4	15
12.	**Set-3**	**292**	**50**	**1.96**	**This work**
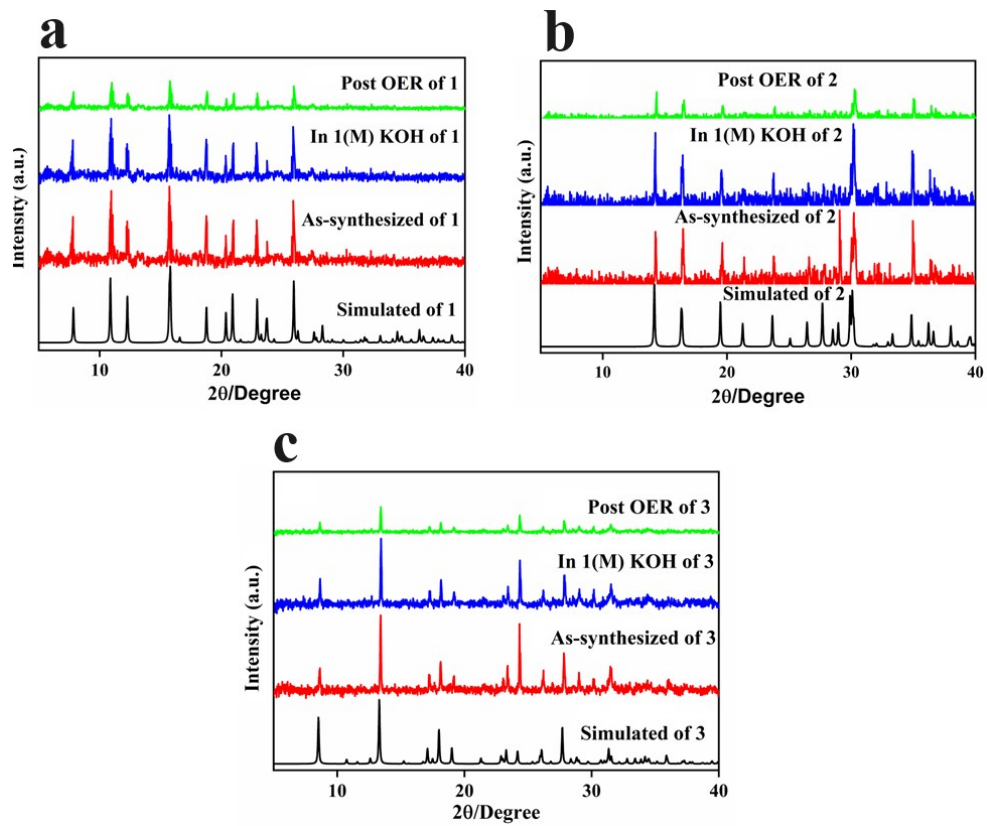
Fig. S9. PXRD of Set-**1 (a)** Set-**2 (b)** Set-**3 (c)** after post OER studies.
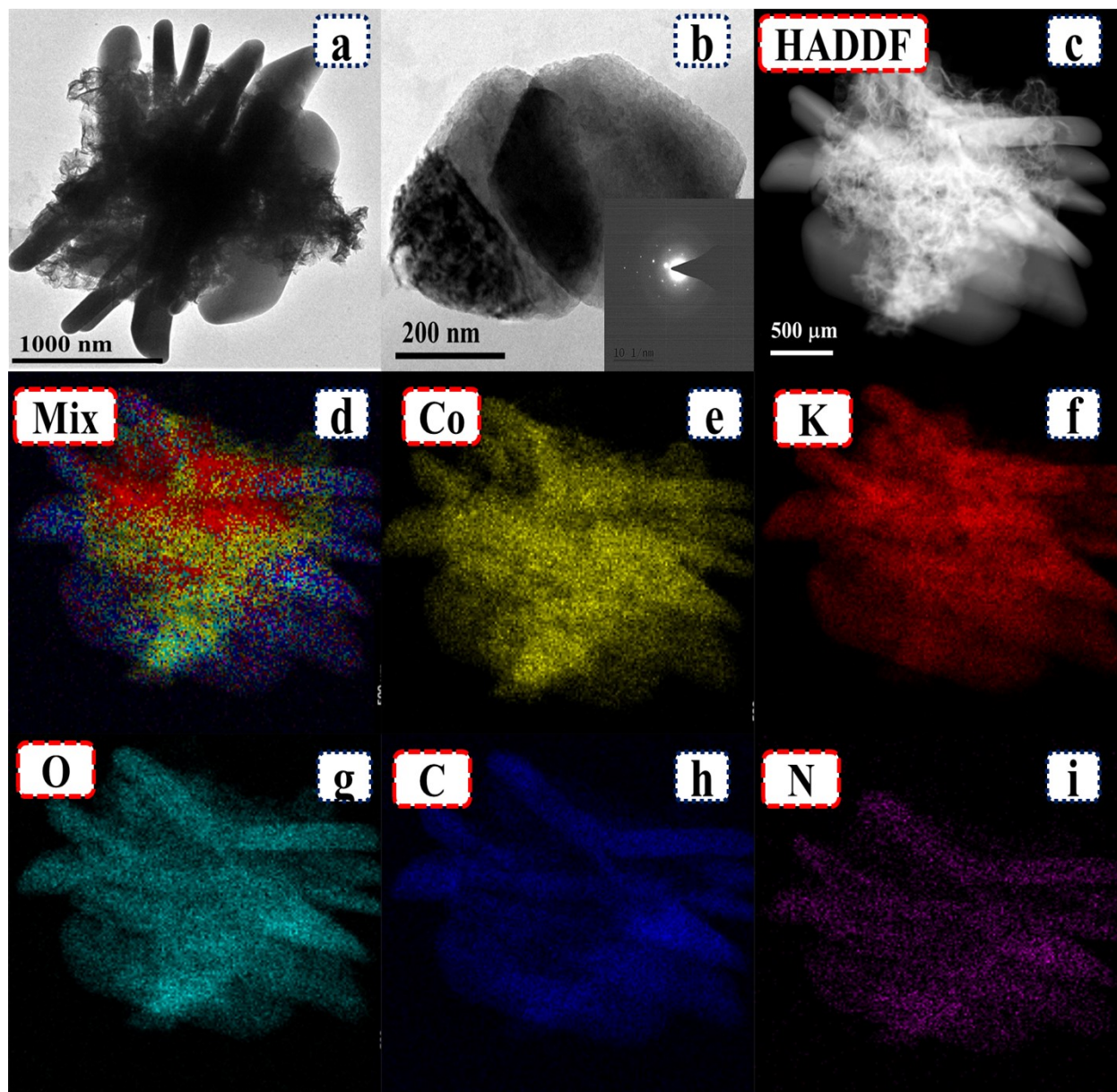
Fig. S10: (a-b) Morphological outcomes of Set-3 catalyst after long-term stability study; inset of **Figure b** portrays the SAED pattern; (c) represented the HADDF area selected for color mapping analysis; (d-i) shows the color mapping results of mix, Co, K, O, C, and N K shell respectively.
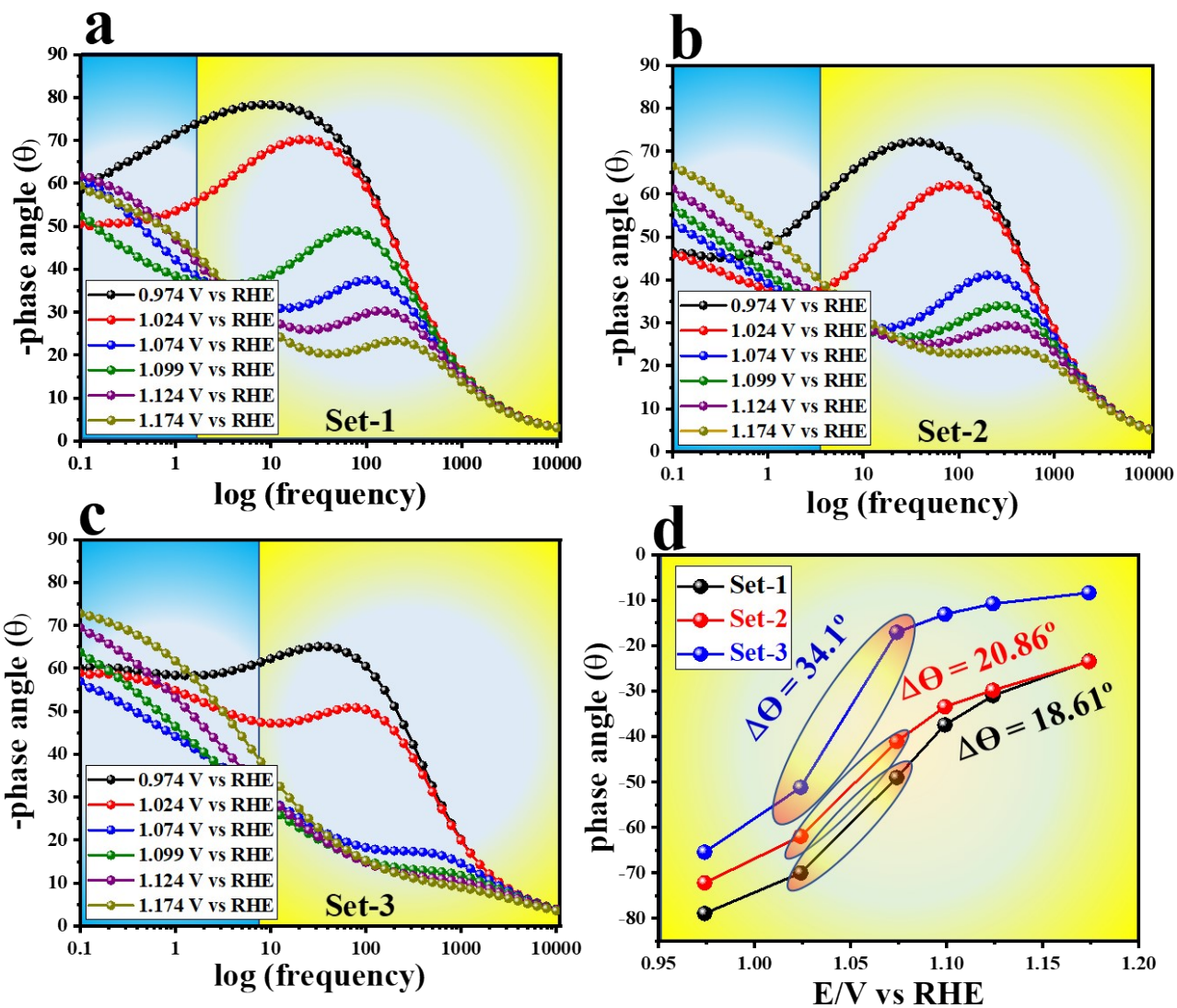
Fig. S11. (a-c) Bode plot for Set-**1**, Set-**2** and Set-**3** compounds at different applied potential value

and (d) Corresponding phase angle information with respect to different applied potential.

References

1. E. Diez-barra, A. De la hoz, A. Sanchez-migallon and J. Tejeda, *Heterocyles(sendai).*, 1992, **34**, 1365-1373.

2. S. -W. Jin and W. -Z. Chen, *Polyhedron*, 2007, **26**, 3074-3084.

3. R. L. Harlow and S. H. Simonsen, *Acta Cryst.*, 1976, **B32**, 466-470.

4. L. C. Nathan and T. D. Mai, *J. Chem. Crystallogr.*, 2000, **30**, 509-518.

5. K. Maity, K. Bhunia, D. Pradhan and K. Biradha, *ACS Appl. Mater. Interfaces*, 2017, **9**, 37548-37553.

6. M. -R. Gao, X. Cao, Q. Gao, Y. -F. Xu, Y. -R. Zheng, J. Jiang and S. -H. Yu, *ACS Nano*, 2014, **8**, 3970-3978.

7. A. Goswami, D. Ghosh, V. V. Chernyshev, A. Dey, D. Pradhan and K. Biradha, *ACS Appl. Mater. Interfaces*, 2020, **12**, 33679.

8. P. Manna, J. Debgupta, S. Bose and S. K. Das, *Angew. Chem. Int. Ed.*, 2016, **55**, 2425-2430.

9. N. Seal, K. Karthick, M. Singh, S. Kundu and S. Neogi, *Chem. Eng. J.*, 2022, **429**, 132301.

10. X. Zhou, X. Shen, Z. Xia, Z. Zhang, J. Li, Y. Ma, Y. Qu, *ACS Appl. Mater. Interfaces*, 2015, **7**, 20322-20331.

11. H. B. Aiyappa, J. Thote, D. B. Shinde, R. Banerjee and S. Kurungot, *Chem. Mater.*, 2016, **28**, 4375-4379.

12. J. Jiang, L. Huang, X. Liu and L. Ai, *ACS Appl. Mater. Interfaces*, 2017, **9**, 7193-7201.

13. S. Gutiérrez-Tarriño, J. L. Olloqui-Sariego, J. J. Calvente, M. Palomino, G. Mínguez Espallargas, J. L. Jordá, F. Rey and P. Oña-Burgos, *ACS Appl. Mater. Interfaces*, 2019, **11**, 46658-46665.

14. S. Wang, Y. Hou, S. Lin and X. Wang, *Nanoscale*, 2014, **6**, 9930-9934.

15. C.-W. Kung, J. E. Mondloch, T. C. Wang, W. Bury, W. Hoffeditz, B. M. Klahr, R. C. Klet, M. J. Pellin, O. K. Farha and J. T. Hupp, *ACS Appl. Mater. Interfaces*, 2015, **7**, 28223-28230.